LETTER

doi:10.1038/nature10428

An olfactory receptor for food-derived odours promotes male courtship in *Drosophila*

Yael Grosjean[1,2], Raphael Rytz[1], Jean-Pierre Farine[2], Liliane Abuin[1], Jérôme Cortot[2], Gregory S. X. E. Jefferis[3] & Richard Benton[1]

Many animals attract mating partners through the release of volatile sex pheromones, which can convey information on the species, gender and receptivity of the sender to induce innate courtship and mating behaviours by the receiver[1]. Male *Drosophila melanogaster* fruitflies display stereotyped reproductive behaviours towards females, and these behaviours are controlled by the neural circuitry expressing male-specific isoforms of the transcription factor Fruitless (FRU^M)[2–5]. However, the volatile pheromone ligands, receptors and olfactory sensory neurons (OSNs) that promote male courtship have not been identified in this important model organism. Here we describe a novel courtship function of Ionotropic receptor 84a (IR84a), which is a member of the chemosensory ionotropic glutamate receptor family[6], in a previously uncharacterized population of FRU^M-positive OSNs. IR84a-expressing neurons are activated not by fly-derived chemicals but by the aromatic odours phenylacetic acid and phenylacetaldehyde, which are widely found in fruit and other plant tissues[7] that serve as food sources and oviposition sites for drosophilid flies[8]. Mutation of *Ir84a* abolishes both odour-evoked and spontaneous electrophysiological activity in these neurons and markedly reduces male courtship behaviour. Conversely, male courtship is increased—in an IR84a-dependent manner—in the presence of phenylacetic acid but not in the presence of another fruit odour that does not activate IR84a. Interneurons downstream of IR84a-expressing OSNs innervate a pheromone-processing centre in the brain. Whereas IR84a orthologues and phenylacetic-acid-responsive neurons are present in diverse drosophilid species, IR84a is absent from insects that rely on long-range sex pheromones. Our results suggest a model in which IR84a couples food presence to the activation of the fru^M courtship circuitry in fruitflies. These findings reveal an unusual but effective evolutionary solution to coordinate feeding and oviposition site selection with reproductive behaviours through a specific sensory pathway.

While mapping the projections of Ionotropic receptor (IR)-expressing OSNs to the primary olfactory centre[9], the antennal lobe, we observed that an *Ir84a* reporter was labelling neurons innervating the VL2a glomerulus. VL2a is one of only three glomeruli that are larger in males and whose OSN inputs and projection neuron outputs express male-specific isoforms of the behavioural sex determination gene *fruitless* (fru^M)[4,5]. fru^M-expressing OSNs have been implicated in promoting male sexual behaviours, because inhibition of synaptic transmission in all of these neurons simultaneously reduces male courtship of females[5]. We confirmed the expression of *Ir84a* in fru^M-expressing neurons by visualizing the co-expression of an *Ir84a* reporter, as well as endogenous *Ir84a* transcripts, with a fru^M reporter[4,5] (Fig. 1a and Supplementary Fig. 1a). No sexual dimorphism was observed either in the number of *Ir84a*-expressing cells (males, 30 ± 2 neurons; females, 30 ± 3 neurons; $n = 4$ antennae each) or in their targeting to VL2a, indicating that FRU^M does not have an essential role in the development of these neurons, similar to other fru^M-expressing OSNs[5].

We generated a *GAL4* knock-in null allele, $Ir84a^{GAL4}$ (Fig. 1b, c). $Ir84a^{GAL4/+}$ heterozygotes expressed a GAL4-responsive, membrane-targeted, green fluorescent protein (GFP) transgene (*UAS-mCD8:GFP*) exclusively in *Ir84a*-expressing OSNs (Fig. 1d, $Ir84a^{+/-}$, and Supplementary Fig. 1b). In $Ir84a^{GAL4}$ homozygotes, the endogenous expression of *Ir84a* was lost, but the distribution and dendritic projections of these neurons, as revealed by mCD8:GFP, was unaffected (Fig. 1d, $Ir84a^{-/-}$). The axons of *Ir84a*-expressing neurons in heterozygous and homozygous $Ir84a^{GAL4}$ flies projected only to VL2a (Fig. 1e). *Ir84a* is therefore dispensable for the specification and wiring of the neurons in which it is expressed. An amino-terminal enhanced GFP (EGFP)-tagged version of this receptor[10] localized to the cell bodies and the ciliated dendritic endings of these neurons but not to their axon termini (Fig. 1f, g), consistent with an exclusive role for IR84a as an olfactory receptor in the fru^M circuitry.

We tested the responses of IR84a-expressing neurons to chemicals produced by male or virgin female flies[11], both by delivering headspaces of flies from a distance (simulating the action of volatile pheromones) and by presenting extracts from fly cuticles at close range (mimicking exposure to non-volatile hydrocarbons, such as contact pheromones[12]). These stimuli produced no or extremely small responses, as detected by extracellular recordings in ac4 sensilla (Supplementary Fig. 2a), which belong to the class of olfactory hair that houses IR84a-expressing neurons, as well as OSNs that express IR75d, or IR76a and IR76b[6]. These observations suggest that IR84a is not tuned to fly-derived pheromones. We therefore tested 163 structurally diverse odours. Only three of these gave responses of >50 spikes s^{-1} above basal activity: phenylacetaldehyde (as identified previously[13]), phenylacetic acid and phenylethylamine (Fig. 2a and Supplementary Fig. 2b). Dose response curves that revealed sensitivity to these ligands are similar in both sexes (Fig. 2b and data not shown).

In $Ir84a^{GAL4}$ homozygous mutants, the responses to phenylacetic acid and phenylacetaldehyde were completely abolished (Fig. 2c, d, $Ir84a^{-/-}$). Re-introduction of *Ir84a* function in these neurons, by using *UAS-Ir84a* or *UAS-EGFP:Ir84a* cDNA transgenes, rescued these phenotypes (Fig. 2c, d, rescue), indicating a cell-autonomous function for IR84a in mediating these odour responses. By contrast, responses to phenylethylamine were unaffected (Fig. 2c, d), corroborating the evidence that this chemical is detected by the neurons that express both IR76a and IR76b[9,10]. Consistent with these loss-of-function data, misexpression of IR84a in Odorant receptor 35a (OR35a)-expressing neurons was sufficient to confer responsiveness to phenylacetic acid and phenylacetaldehyde (Supplementary Fig. 2c). The basal activity in *Ir84a* mutant ac4 sensilla was also lower than that in the ac4 sensilla of wild-type and rescue genotypes (Fig. 2e, f), indicating that IR84a has a role in promoting spontaneous firing.

Phenylacetic acid and phenylacetaldehyde are aromatic compounds found in a diverse range of fruit and other plant tissues[7], as well as in their fermentation products[14], and they are used in human perfumes for their floral, honey-like, sweet smell. We confirmed the presence of these chemicals in two host fruit for drosophilid flies[8], overripe bananas and

[1]Center for Integrative Genomics, Faculty of Biology and Medicine, University of Lausanne, CH-1015 Lausanne, Switzerland. [2]Centre des Sciences du Goût et de l'Alimentation, UMR-6265 CNRS, UMR-1324 INRA, Université de Bourgogne, 6 Boulevard Gabriel, 21000 Dijon, France. [3]Division of Neurobiology, MRC Laboratory of Molecular Biology, Cambridge CB2 0QH, UK.

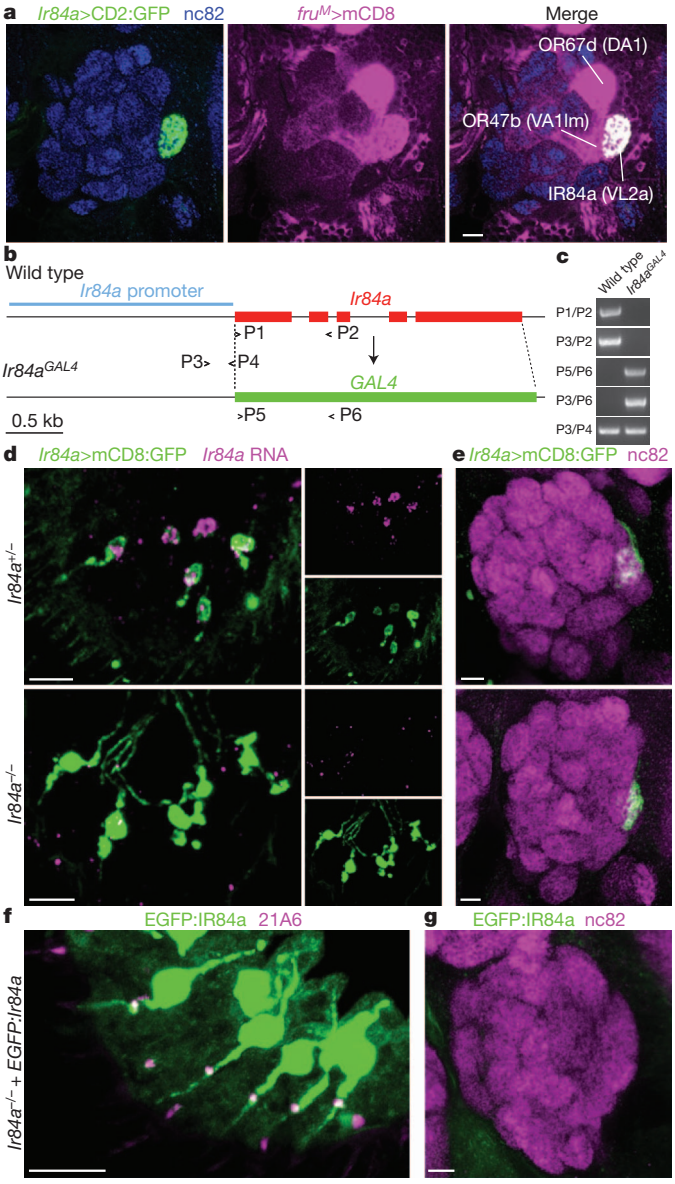

Figure 1 | Gene targeting of *Ir84a*, a candidate olfactory receptor in the *fru*^{M} circuit. **a**, Immunofluorescence using anti-GFP (green), anti-CD8 (magenta) and nc82 (blue; neuropil marker) antibodies on an antennal lobe of an animal in which an *Ir84a* promoter-*lexA* transgene drives (>) expression of a LexA-responsive CD2:GFP reporter transgene and in which the *fru*^{M} GAL4 insertion allele drives expression of a GAL4-responsive CD8 reporter transgene (genotype, *Ir84a-lexA/UAS-mCD8;lexAop-rCD2:GFP/fru*^{GAL4}). **b**, Schematic of the *Ir84a* locus, illustrating the organization of wild-type *Ir84a* and null mutant *Ir84a*^{GAL4} alleles. The span of the cloned *Ir84a* promoter is also indicated. P denotes PCR primer position. kb, kilobases. **c**, PCR confirmation of the *Ir84a*^{GAL4} allele using the pairs of primers shown in **b**. **d**, Combined *Ir84a* RNA *in situ* hybridization (magenta) and anti-GFP immunofluorescence (green) on antennae from *Ir84a* mutant flies: top, heterozygous mutants (*UAS-mCD8:GFP/+;Ir84a*^{GAL4}*/+*); and, bottom, homozygous mutants (*UAS-mCD8:GFP/+;Ir84a*^{GAL4}*/Ir84a*^{GAL4}). Separate channels are shown on the right. **e**, Immunofluorescence using anti-GFP (green) and nc82 (magenta) antibodies on antennal lobes from *Ir84a* mutant flies: top, control heterozygous mutants (*UAS-mCD8:GFP;Ir84a*^{GAL4}*/+*); and, bottom, homozygous mutants (*UAS-mCD8:GFP;Ir84a*^{GAL4}*/Ir84a*^{GAL4}). **f**, Immunofluorescence using anti-GFP antibodies (green) and antibodies specific for the sensory cilium base marker 21A6 (magenta) on an antenna expressing EGFP:IR84a (*UAS-EGFP:Ir84a/+;Ir84a*^{GAL4}*/Ir84a*^{GAL4}). **g**, Immunofluorescence using anti-GFP (green) and nc82 (magenta) antibodies on an antennal lobe of a fly expressing EGFP:IR84a (*UAS-EGFP:Ir84a;Ir84a*^{GAL4}*/Ir84a*^{GAL4}). **a**, **d**–**g**, Scale bar, 10 μm.

the prickly-pear cactus *Opuntia ficus-indica*, as well as in laboratory *Drosophila* medium, by using gas chromatography–mass spectrometry analysis (Supplementary Table 1). The ubiquity of phenylacetic acid in vegetal tissues may be linked with its activity as a growth-regulating auxin[7] and/or its production by plant-associated microorganisms[15]. Small, but reproducible, quantities of phenylacetic acid and phenylacetaldehyde were also detected in whole-body cuticular extracts of male and virgin female *D. melanogaster* (Supplementary Table 1). The similarity in the relative amounts of these chemicals in laboratory medium and fruitfly extracts (Supplementary Table 1) suggested that these chemicals are transferred from food to flies during their culture. 'Clean' cuticular extracts from animals grown on a minimal medium containing only sucrose and agarose consistently contain no detectable phenylacetaldehyde or phenylacetic acid (Supplementary Table 1).

The expression of IR84a in *fru*^{M}-expressing neurons implicates this receptor in the regulation of male courtship[4,5]. Indeed, in single-pair courtship assays, we observed that *Ir84a*^{GAL4} mutant males court wild-type females significantly less than do wild-type males (Fig. 3a and Supplementary Fig. 3a, b). This phenotype was observed using both decapitated virgin females (which do not produce feedback signals) (Fig. 3a) and in more natural conditions, with intact females together with food (Supplementary Fig. 3b). Most individual components of the courtship ritual were affected in *Ir84a* mutant flies (Supplementary Fig. 3a). These defects were rescued with a *UAS-Ir84a* transgene, confirming that they result from the absence of IR84a in OSNs (Fig. 3a and Supplementary Fig. 3a, b). The observed reduction in male heterosexual courtship index (~50%) is highly comparable to the phenotype of flies in which all FRU^{M}-positive OSNs are silenced[5], suggesting that IR84a-expressing neurons are the major olfactory *fru*^{M} channel contributing to this behaviour. Residual courtship is presumably stimulated by other sensory modalities, such as taste[16,17]. Male wild-type *D. melanogaster* also show a low level of courtship towards other males, and we found that this homosexual courtship was also markedly reduced in *Ir84a*^{GAL4} mutants (Fig. 3b). By contrast, *Ir84a*^{GAL4} mutant females did not show overt defects in reproductive behaviours, including copulation latency, success or duration (Fig. 3c).

In innate olfactory preference assays, *Ir84a*^{GAL4} mutant flies still show robust avoidance of acetic acid, indicating that they do not have a general impairment in sensory detection (Supplementary Fig. 3c). By contrast, we did not observe any obvious responses of flies to phenylacetic acid (Supplementary Fig. 3d), suggesting that this food-derived odour is not a volatile stimulus that attracts flies but is a salient cue at close range. Notably, phenylacetic acid has a low vapour pressure (~0.005 mm Hg at 25 °C) compared with other fruit volatiles (for example, ethyl butyrate, which has a vapour pressure of 15 mm Hg at 25 °C). The observation that courtship is reduced in *Ir84a*^{GAL4} mutants in assays in which only small amounts of phenylacetic acid are present on fly cuticles (Supplementary Table 1) raises the possibility that spontaneous activity of these neurons also contributes to establishing a basal courtship level, which is abolished in the absence of IR84a (Fig. 2e, f).

To test whether IR84a ligands are sufficient to promote courtship, we adapted our assay by using killed female objects (which males court at only low levels) and by replacing the base of the chamber with gauze, beneath which we placed a filter paper treated with odour or solvent. Perfuming with phenylacetic acid nearly doubled the courtship index of wild-type flies compared with a solvent control (Fig. 3d). This effect was abolished in *Ir84a*^{GAL4} mutants and could be restored, albeit not fully, by introducing a *UAS-Ir84a* transgene. By contrast, ethyl butyrate, which does not activate IR84a (Supplementary Fig. 2b), did not increase courtship (Fig. 3d). We also perfumed the courtship chamber with *Drosophila* food—which contains phenylacetic acid (Supplementary Table 1)—and observed that this complex olfactory stimulus induced IR84a-dependent increases in male courtship behaviour (Fig. 3e).

The other *fru*^{M}-expressing OSN populations express either OR67d, which is a receptor for the antiaphrodisiac male pheromone

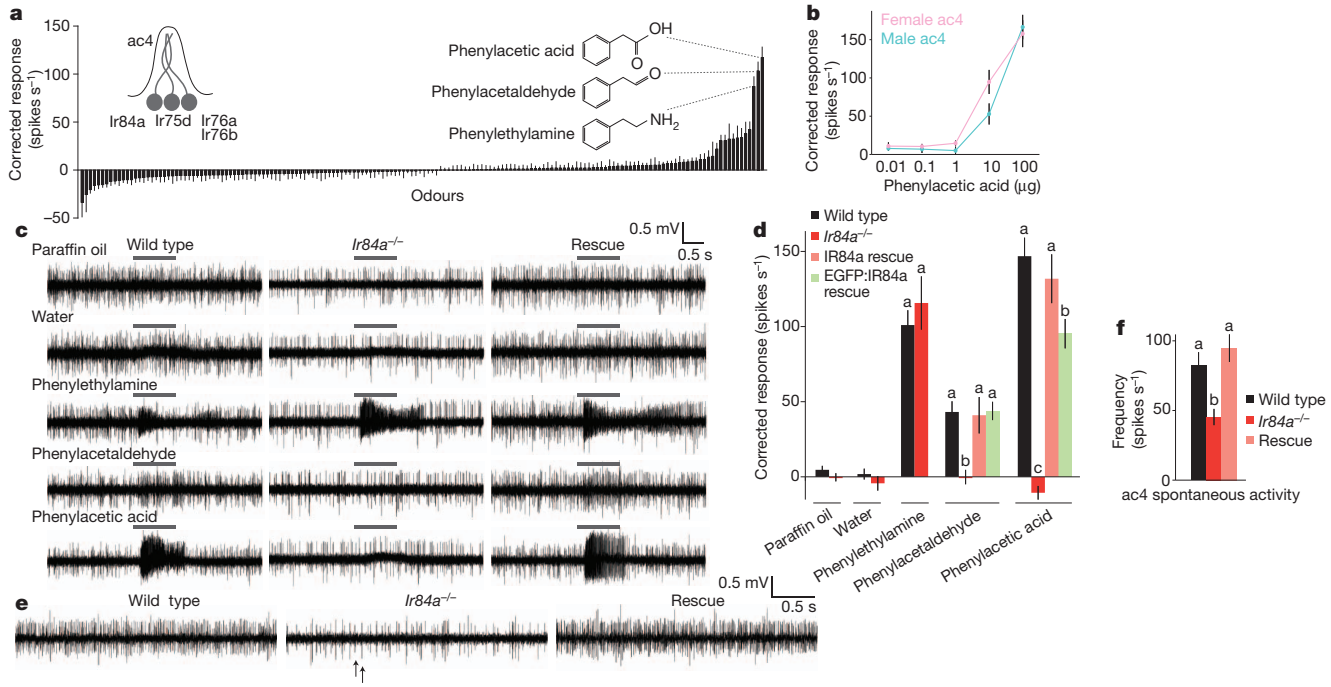

Figure 2 | Essential requirement for IR84a for spontaneous and odour-evoked neuronal responses. **a**, An odour ligand screen in ac4 sensilla. The mean evoked responses of ac4 sensilla neurons to a panel of 163 odours (representing the summed activities of the IR84a-expressing, IR75d-expressing, and IR76a- plus IR76b-expressing neurons). Data are presented as mean ± s.e.m.; $n \geq 4$, mixed genders. An enlarged version of this histogram with all of the odour names indicated is provided in Supplementary Fig. 2b. The structures of the best three agonists are shown. **b**, The dose response curve to phenylacetic acid of male and female ac4 sensilla. Data are presented as mean ± s.e.m.; $n = 12$ for each gender. The doses reflect the total mass of phenylacetic acid (diluted in solvent) in the odour syringe. The responses of the male and female sensilla are not significantly different at any concentration (analysis of variance (ANOVA), $P > 0.0571$). A higher concentration of phenylacetic acid could not be prepared because of its limited solubility. **c**, Representative traces of recordings of ac4 sensilla stimulated with the indicated odour stimuli (10 µl phenylacetic acid (10 µg µl^{-1}) or 10 µl (1% (v/v)) other odours) in wild-type (w^{1118}), $Ir84a^{-/-}$ mutant ($Ir84a^{GAL4}/Ir84a^{GAL4}$) and IR84a rescue (*UAS-Ir84a/+;*$Ir84a^{GAL4}/Ir84a^{GAL4}$) flies. Paraffin oil and water are solvent controls. The grey bars above the traces mark the stimulus time (1 s). **d**, Quantification of mean responses to the indicated odours for the experiment shown in **c**. Data are presented as mean ± s.e.m.; $n \geq 11$, mixed genders. The restoration of phenylacetaldehyde and phenylacetic acid responses by the expression of EGFP:IR84a (*UAS-EGFP:Ir84a/+;*$Ir84a^{GAL4}/Ir84a^{GAL4}$) is also shown (green). For each odour stimulus, bars labelled with different letters are significantly different from each other (phenylethylamine ANOVA, $P = 0.4861$; phenylacetaldehyde ANOVA, $P = 0.0003$; phenylacetic acid ANOVA, $P < 0.0001$). For phenylacetic acid, EGFP:IR84a rescue is partial. **e**, Representative traces of spontaneous activity in ac4 sensilla in wild-type, $Ir84a^{-/-}$ mutant ($Ir84a^{GAL4}/Ir84a^{GAL4}$) and IR84a rescue (*UAS-Ir84a/+;*$Ir84a^{GAL4}/Ir84a^{GAL4}$) flies. The arrows mark two distinct spike amplitudes discernible in the sparser spike trains in *Ir84a* mutant sensilla; these are likely to correspond to the IR75d- and the IR76a- plus IR76b-expressing neurons. **f**, Quantification of the mean spontaneous activity in ac4 sensilla in the experiment shown in **e**. Data are presented as mean ± s.e.m.; $n \geq 12$, mixed genders. Bars labelled with different letters are significantly different (ANOVA, $P = 0.0005$).

cis-vaccenyl acetate[18], or OR47b, which is activated by unidentified fly-derived odours from both sexes[11] and may participate in mate localization[19,20]. We examined how IR84a sensory information is integrated with these pheromonal pathways, by visualizing the axons of projection neurons innervating the VL2a (IR84a), VA1lm (OR47b) and DA1 (OR67d) glomeruli, which carry sensory information to the mushroom body and lateral horn[21] (Fig. 4a). We registered images of single-labelled projection neurons of different glomerular classes onto a common reference brain (see Methods). DA1 and VA1lm excitatory projection neurons target an anterior-ventral pheromone-processing region of the lateral horn[22], which is segregated from projection neurons that are responsive to general food odours[22]. Importantly, we found that VL2a projection neurons—and no other IR-expressing projection neuron class[9]—are highly interdigitated with pheromone pathways and not food pathways (Fig. 4a, b). Indeed, VL2a projection neuron axon terminals overlap more strongly with VA1lm projection neurons than any of the other 44 projection neuron classes (see Methods and Supplementary Fig. 4b, c), consistent with projection neurons of both of these classes transmitting courtship-promoting sensory signals[19,20]. The VL2a, DA1 and VA1lm inhibitory projection neurons were observed to overlap to a similar extent (Supplementary Fig. 4a–c). The anatomical convergence of combinations of excitatory and inhibitory inputs from VL2a, VA1lm and DA1 projection neurons may allow the integration of olfactory signals by fru^M-expressing third-order neurons[23,24] to control male courtship behaviour.

Many olfactory IRs are conserved in insects[25] and may detect odours that are important for all species. By contrast, although IR84a orthologues are present in ecologically diverse drosophilids, they are absent from other Diptera and more divergent insects (Supplementary Fig. 5a). In the cactophilic species *Drosophila mojavensis*, we identified coeloconic sensilla with neurons that are responsive to phenylacetic acid and phenylacetaldehyde on their anterior antennal surface (similar to ac4 sensilla in *D. melanogaster*) (Supplementary Fig. 5b). Thus, IR84a may have a conserved, drosophilid-specific function.

Despite the widely held assumption of the existence of volatile chemicals that promote courtship in *Drosophila*[4,5], behavioural evidence for long-range pheromones is inconclusive[26,27], and no female-specific volatile compound that activates male OSNs has been identified[11]. Our characterization of IR84a identifies an olfactory receptor that is expressed in FRU^M-positive neurons and is required to promote male courtship. Surprisingly, this receptor is not activated by fly-derived odours but rather by aromatic compounds that are present in the vegetal substrates in which fruitflies feed, breed and oviposit[8]. Thus, the IR84a pathway may promote male courtship in the presence of food, complementing the functions of pheromone receptors in regulating mate choice (Supplementary Fig. 5c). This model can account for

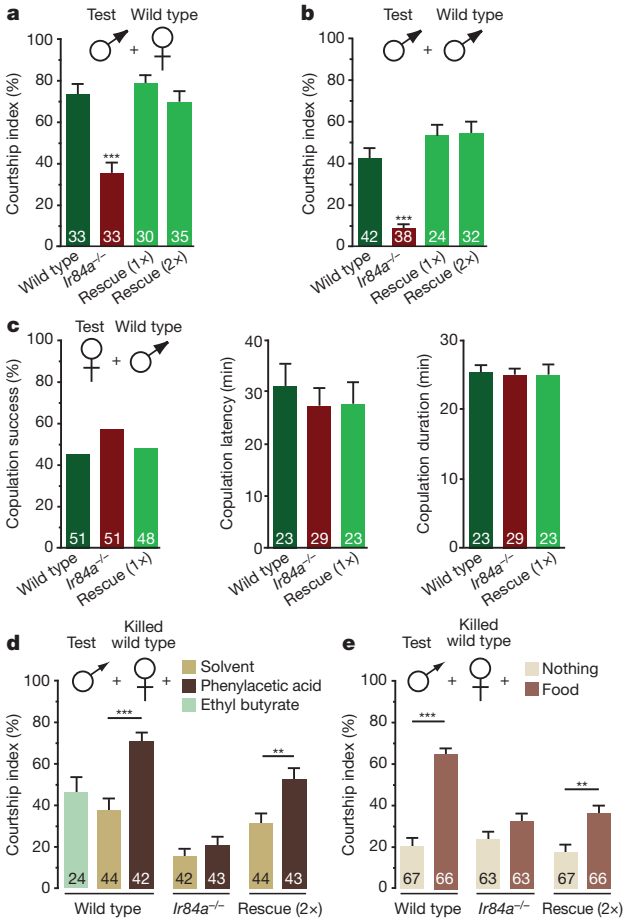

Figure 3 | IR84a is required for male courtship behaviour. **a**, Courtship indices for wild-type (w^{1118}), $Ir84a^{-/-}$ mutant ($Ir84a^{GAL4}/Ir84a^{GAL4}$) and IR84a rescue (rescue (1×), *UAS-Ir84a/+*;$Ir84a^{GAL4}/Ir84a^{GAL4}$; or rescue (2×), *UAS-Ir84a/UAS-Ir84a*;$Ir84a^{GAL4}/Ir84a^{GAL4}$) male flies paired with wild-type decapitated virgin females. Data are presented as mean ± s.e.m.; *n* is shown in the corresponding bar in this and other histograms. **b**, Courtship indices for male flies of the indicated genotypes (as in **a**) paired with wild-type decapitated males. Data are presented as mean ± s.e.m. **c**, Receptivity of female flies of the indicated genotypes to wild-type males as measured by percentage copulation success (left), copulation latency (centre) and copulation duration (right). Data are presented as mean ± s.e.m. **d**, **e**, Courtship indices for male flies paired with freeze-killed wild-type virgin females in an assay chamber perfumed from beneath a mesh (to avoid direct contact with the flies) with solvent (paraffin oil), phenylacetic acid or ethyl butyrate (**d**) or nothing or fly food (**e**). Data are presented as mean ± s.e.m. Statistical analysis was performed as follows. **a**, **b**, A one-way ANOVA (Kruskal–Wallis, $P < 0.0001$) followed by Dunn's multiple comparison post hoc test, in which all genotypes are individually compared with the control, was performed on all data. ***, $P < 0.001$. **c**, Values for percentage female copulation success were compared using a chi-squared statistical test. For copulation latency and duration, a one-way ANOVA (Kruskal–Wallis) followed by Dunn's multiple comparison post hoc test were performed; no significant differences between genotypes were found. **d**, **e**, A two-way ANOVA, followed by a Bonferroni post-hoc test, was performed on all data, except for ethyl butyrate: $P < 0.0001$ for the odour stimulus, and $P < 0.0001$ for the genotype as source of variation; $P < 0.0001$ for the interaction between the two sources of variation, confirming a link between odour and genotype. **, $P < 0.01$; ***, $P < 0.001$. Ethyl butyrate was compared to paraffin oil using a Mann–Whitney *U* test and yielded no statistical difference for control males. Although the rescue genotype displays a significant difference between phenylacetic acid (or food) and control perfuming treatments, its courtship indices are lower than those of the control genotype; this may result from lower levels of IR84a expression in the rescue animals or from indirect effects such as genetic background.

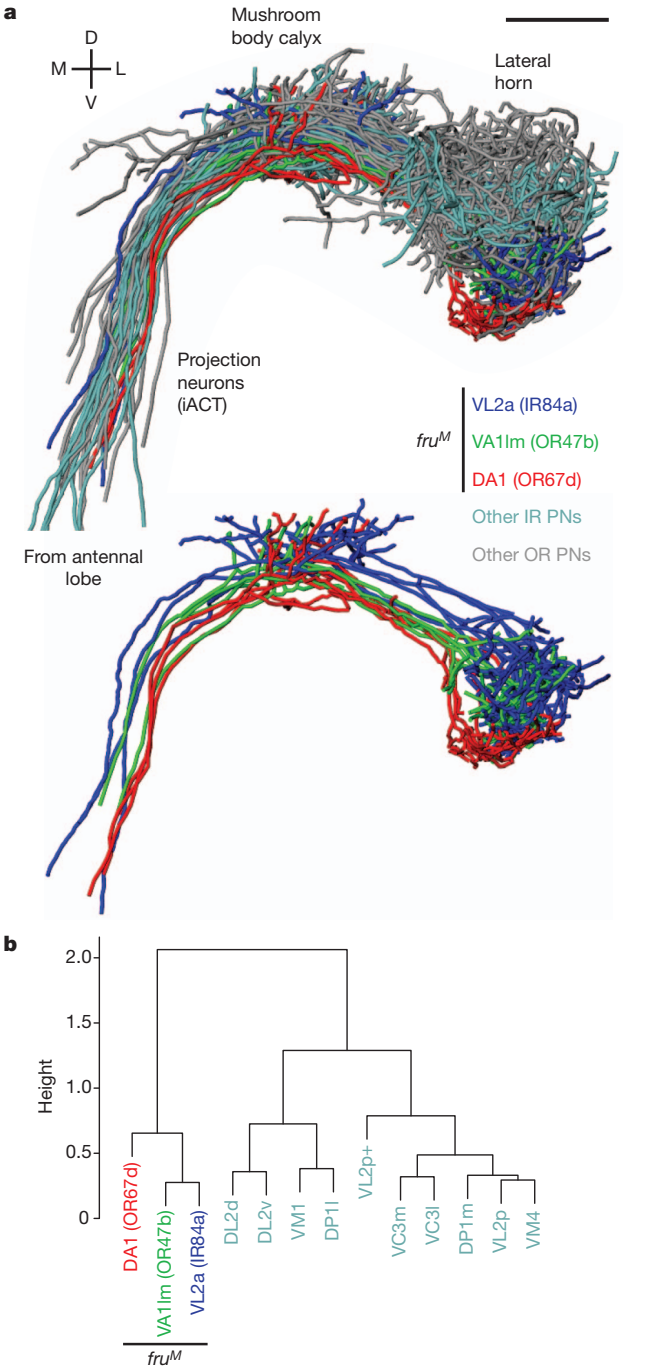

Figure 4 | Anatomical integration of VL2a (IR84a-expressing) projection neurons in the pheromone processing centre. **a**, Top, three-dimensional rendering of registered axonal projections of projection neurons (PNs) receiving input from the VL2a glomerulus (IR84a-expressing) (dark blue), the VA1lm glomerulus (OR47b-expressing) (green) and the DA1 glomerulus (OR67d-expressing) (red) ($n = 4$ for each class). Other classes of projection neuron are shown in cyan (nine IRs[9]) and grey (27 ORs[22]) ($n = 1$ for each class). These projection neurons are cholinergic and project to both the mushroom body and the lateral horn through the inner antennocerebral tract (iACT); a small minority of other projection neurons are GABAergic (γ-aminobutyric acid-containing) and project exclusively to the lateral horn through the middle ACT (Supplementary Fig. 4a). Bottom, when the other projection neurons are removed, the extensive co-mingling of VL2a and VA1lm projection neurons is evident. Scale bar, 25 μm. D, dorsal; L, lateral; M, medial; V, ventral. **b**, Cluster analysis of normalized axon overlap scores (*y* axis) using Ward's method (see Methods) demonstrates that VL2a projection neurons cluster with projection neurons from other fru^M-expressing glomeruli rather than with other IR-expressing projection neurons. Colours are as in **a**.

the widespread observations that *D. melanogaster* and other drosophilids mate predominantly on their food substrates[8,28]. Whereas many insects and other animal classes use long-range sex pheromones to attract potential mates[1], the evolution of IR84a in fruitflies has provided an alternative (although not necessarily exclusive) olfactory mechanism to unite males with females by integrating food-sensing neurons with the circuitry controlling sexual behaviour. Whether other animals have dedicated sensory pathways for environmental 'aphrodisiacs' remains an open question.

METHODS SUMMARY

Genetic and molecular biological manipulations and histological and electrophysiological analyses were performed essentially as described previously[6,9,10]. Responses to *Drosophila*-derived stimuli were measured by adapting previous protocols[11]. *Drosophila* extracts and food or fruit extracts were made using CH_2Cl_2 solvent and were analysed by gas chromatography–mass spectrometry on a GC-MS-QP2010 apparatus (Shimadzu). Courtship tests were performed at 25 °C in round observation chambers (1.2 cm in diameter and 0.4 cm deep) under far-red light and were video recorded and annotated manually by observers who were blinded to the genotypes. For perfumed behavioural assays, the courtship chamber was placed on top of an identical chamber, with the chambers separated by muslin gauze to avoid contact between the flies in the top chamber and the chemical stimuli placed in the bottom chamber. Olfactory responses were measured using a Y-maze assay. Projection neurons from several sources (see Methods) were traced, where necessary, using Amira software (http://www.amira.com) and registered, by adapting previous approaches[22]. The degree of overlap between the axon terminals of different projection neurons was measured using the three-dimensional convex hull formed by each set of terminals. Cluster analysis of these data was performed using Ward's method.

Full Methods and any associated references are available in the online version of the paper at www.nature.com/nature.

Received 4 June 2010; accepted 3 August 2011.
Published online 28 September 2011.

1. Wyatt, T. D. *Pheromones and Animal Behaviour: Communication by Smell and Taste* (Oxford Univ. Press, 2003).
2. Dickson, B. J. Wired for sex: the neurobiology of *Drosophila* mating decisions. *Science* **322,** 904–909 (2008).
3. Demir, E. & Dickson, B. J. *fruitless* splicing specifies male courtship behavior in *Drosophila. Cell* **121,** 785–794 (2005).
4. Manoli, D. S. *et al.* Male-specific *fruitless* specifies the neural substrates of *Drosophila* courtship behaviour. *Nature* **436,** 395–400 (2005).
5. Stockinger, P., Kvitsiani, D., Rotkopf, S., Tirian, L. & Dickson, B. J. Neural circuitry that governs *Drosophila* male courtship behavior. *Cell* **121,** 795–807 (2005).
6. Benton, R., Vannice, K. S., Gomez-Diaz, C. & Vosshall, L. B. Variant ionotropic glutamate receptors as chemosensory receptors in *Drosophila. Cell* **136,** 149–162 (2009).
7. Wightman, F. & Lighty, D. L. Identification of phenylacetic acid as a natural auxin in the shoots of higher plants. *Physiol. Plant.* **55,** 17–24 (1982).
8. Markow, T. A. & O'Grady, P. Reproductive ecology of *Drosophila. Funct. Ecol.* **22,** 747–759 (2008).
9. Silbering, A. F. *et al.* Complementary function and integrated wiring of the evolutionarily distinct *Drosophila* olfactory subsystems. *J. Neurosci.* doi:10.1523/JNEUROSCI.2360-11.2011 (21 September 2011).
10. Abuin, L. *et al.* Functional architecture of olfactory ionotropic glutamate receptors. *Neuron* **69,** 44–60 (2011).
11. van der Goes van Naters, W. & Carlson, J. R. Receptors and neurons for fly odors in *Drosophila. Curr. Biol.* **17,** 606–612 (2007).
12. Ferveur, J. F. Cuticular hydrocarbons: their evolution and roles in *Drosophila* pheromonal communication. *Behav. Genet.* **35,** 279–295 (2005).
13. Yao, C. A., Ignell, R. & Carlson, J. R. Chemosensory coding by neurons in the coeloconic sensilla of the *Drosophila* antenna. *J. Neurosci.* **25,** 8359–8367 (2005).
14. Barata, A. *et al.* Analytical and sensorial characterization of the aroma of wines produced with sour rotten grapes using GC-O and GC-MS: identification of key aroma compounds. *J. Agric. Food Chem.* **59,** 2543–2553 (2011).
15. Kim, J., Jeon, C. O. & Park, W. A green fluorescent protein-based whole-cell bioreporter for the detection of phenylacetic acid. *J. Microbiol. Biotechnol.* **17,** 1727–1732 (2007).
16. Bray, S. & Amrein, H. A putative *Drosophila* pheromone receptor expressed in male-specific taste neurons is required for efficient courtship. *Neuron* **39,** 1019–1029 (2003).
17. Kohatsu, S., Koganezawa, M. & Yamamoto, D. Female contact activates male-specific interneurons that trigger stereotypic courtship behavior in *Drosophila. Neuron* **69,** 498–508 (2011).
18. Kurtovic, A., Widmer, A. & Dickson, B. J. A single class of olfactory neurons mediates behavioural responses to a *Drosophila* sex pheromone. *Nature* **446,** 542–546 (2007).
19. Root, C. M. *et al.* A presynaptic gain control mechanism fine-tunes olfactory behavior. *Neuron* **59,** 311–321 (2008).
20. Wang, L. *et al.* Hierarchical chemosensory regulation of male–male social interactions in *Drosophila. Nature Neurosci.* **14,** 757–762 (2011).
21. Vosshall, L. B. & Stocker, R. F. Molecular architecture of smell and taste in *Drosophila. Annu. Rev. Neurosci.* **30,** 505–533 (2007).
22. Jefferis, G. S. *et al.* Comprehensive maps of *Drosophila* higher olfactory centers: spatially segregated fruit and pheromone representation. *Cell* **128,** 1187–1203 (2007).
23. Cachero, S., Ostrovsky, A. D., Yu, J. Y., Dickson, B. J. & Jefferis, G. S. Sexual dimorphism in the fly brain. *Curr. Biol.* **20,** 1589–1601 (2010).
24. Yu, J. Y., Kanai, M. I., Demir, E., Jefferis, G. S. & Dickson, B. J. Cellular organization of the neural circuit that drives *Drosophila* courtship behavior. *Curr. Biol.* **20,** 1602–1614 (2010).
25. Croset, V. *et al.* Ancient protostome origin of chemosensory ionotropic glutamate receptors and the evolution of insect taste and olfaction. *PLoS Genet.* **6,** e1001064 (2010).
26. Ewing, A. W. & Manning, A. The effect of exogenous scent on the mating of *Drosophila melanogaster. Anim. Behav.* **11,** 596–598 (1963).
27. Shorey, H. H. & Bartell, R. J. Role of a volatile female sex pheromone in stimulating male courtship behaviour in *Drosophila melanogaster. Anim. Behav.* **18,** 159–164 (1970).
28. Spieth, H. T. Courtship behavior in *Drosophila. Annu. Rev. Entomol.* **19,** 385–405 (1974).

Supplementary Information is linked to the online version of the paper at www.nature.com/nature.

Acknowledgements We are grateful to B. Dickson, A. Hofbauer, T. Lee, the Bloomington *Drosophila* Stock Center, the *Drosophila* Species Stock Center and the Developmental Studies Hybridoma Bank for provision of plasmid vectors, *Drosophila* strains and antibodies. We are also grateful to A. Wong, J. Wang, R. Axel, H.-H. Yu and T. Lee for sharing raw image data. We thank D. Featherstone, J.-F. Ferveur, T. Kawecki, L. Keller, S. Martin and members of the Benton laboratory for comments on the manuscript. Y.G., J.-P.F. and J.C. are supported by the Centre National de la Recherche Scientifique (CNRS), the Agence Nationale de la Recherche (ANR; JCJC, GGCB-2010) and the Conseil Régional de Bourgogne (FABER). R.R. was supported by a Roche Research Foundation fellowship. G.S.X.E.J. is supported by the Medical Research Council and a European Research Council Starting Investigator Grant. Research in R.B.'s laboratory is supported by the University of Lausanne, a European Research Council Starting Independent Researcher Grant and the Swiss National Science Foundation.

Author Contributions Y.G. and R.B. conceived the project. Y.G. performed the gene-targeting screen, contributed to the histological analysis and performed most of the behavioural experiments. R.R. performed the electrophysiological odour response screen, the fly odour stimulation assays and the phylogenetic analyses. J.-P.F. performed the chemical analysis. L.A. assisted in the generation and characterization of transgenic flies and contributed to the histological analysis. J.C. contributed to the behavioural experiments. G.S.X.E.J. performed the analysis of projection neurons. R.B. generated the DNA constructs, performed all other electrophysiological analyses and wrote the paper with contributions from Y.G., R.R., J.-P.F. and G.S.X.E.J.

Author Information Reprints and permissions information is available at www.nature.com/reprints. The authors declare no competing financial interests. Readers are welcome to comment on the online version of this article at www.nature.com/nature. Correspondence and requests for materials should be addressed to R.B. (Richard.Benton@unil.ch).

METHODS

***Drosophila* strains.** *Drosophila* stocks were maintained on a standard corn flour, yeast and agar medium under a 12 h light and 12 h dark cycle at 25 °C. We used the following mutant and transgenic strains: *Or35a-GAL4* (ref. 13), *Ir84a-GAL4* (ref. 9), *UAS-Ir84a*[6], *UAS-EGFP:Ir84a*[10], *UAS-mCD8:GFP*[29], *fru*^{GAL4} (ref. 5), *fruP1-GAL4* (ref. 4), *lexAop-rCD2::GFP*, *UAS-mCD8* (ref. 30), *UAS-DTI*[31], *70FLP,70I-SceI/Cyo*, *70FLP* and *70I-CreI*[32]. For behavioural analysis, all flies carrying mutant and transgenic chromosomes were backcrossed to an isogenized w^{1118} control line for five generations. The sequenced wild-type *D. melanogaster* strain (Bloomington *Drosophila* Stock Center number 2057) was used for the ac4 odour screen, and Canton-S was used as the courtship object in behavioural experiments. Wild-type *D. mojavensis* was obtained from the *Drosophila* Species Stock Center (University of California, San Diego; stock number 15081-1352.22).

Molecular biology. New transgenes were constructed as follows, using standard methods. For the *Ir84a GAL4* targeting construct, 5,087 base pairs (bp) genomic DNA immediately upstream of the *Ir84a* start codon was amplified and subcloned as 1,924-bp and 3,163-bp fragments either side of the I-SceI site upstream of *GAL4* in the pED36 targeting vector[3]. Similarly, a 964-bp genomic fragment immediately downstream of the *Ir84a* stop codon was cloned downstream of *GAL4*. For the *Ir84a* promoter-*lexA* construct, the same 1,964 bp *Ir84a* promoter fragment used in the *Ir84a-GAL4* transgene[9] was cloned upstream of *lexA:VP16-SV40* (ref. 30) in the vector pattB[33].

Gene targeting. Targeted replacement of *Ir84a* by *GAL4* was performed essentially as described previously[18]. A transgenic line containing the *Ir84a GAL4* targeting construct on the X chromosome was used as a donor for targeting crosses in which heat-shock-inducible transgenic FLP and I-SceI enzymes were used to excise and linearize the targeting fragment. Reinsertion was detected by the presence of a FLP-insensitive *white*$^{+}$ marker. From ~193,000 flies screened, five targeted insertions were recovered and verified by PCR as duplicates of the *Ir84a* locus. One duplicate was resolved with I-CreI, selecting for loss of *white*$^{+}$. From 218 *white*$^{-}$ flies, 1 was found to contain the desired precise *Ir84a* to *GAL4* replacement.

Histology. Immunofluorescence on antennal cryosections was performed as described previously[10,34]. Immunofluorescence on whole mount brains, and combined fluorescent RNA *in situ* hybridization and immunofluorescence on antennal sections, was performed as described previously[9]. The primary antibodies used were mouse monoclonal nc82 (1:10 dilution; provided by A. Hofbauer), mouse monoclonal 21A6 (1:200; Developmental Studies Hybridoma Bank), rabbit anti-GFP (1:1,000; Invitrogen), mouse anti-GFP (1:500; Invitrogen), rat anti-mCD8 (1:50; Caltag), anti-DIG-POD (1:500; Roche). The secondary antibodies used were Alexa Fluor 488-, Cy3- and Alexa Fluor 647-conjugated goat anti-mouse, anti-rabbit or anti-rat IgG (Molecular Probes and Jackson ImmunoResearch). These were diluted to 1:100 and 1:1,000 for whole mount brains and antennal sections, respectively. All microscopy was performed using an LSM 510 laser scanning confocal microscope (Zeiss).

Electrophysiology. Extracellular recordings in single sensilla of 1–8-day-old flies were performed and quantified as described previously[6]. Odours were diluted to 1% (v/v) unless otherwise noted. The CAS numbers, solvents, sources and purities for the odorants used are provided in Supplementary Table 2. Corrected responses were quantified by counting all spikes in ac4 sensilla in a 0.5 s window from 150–200 ms after the stimulus trigger. This delay period was defined precisely for each recording session with a control odour response and mainly represents the time for the odour to reach the preparation. From this spike value, we subtracted the number of spontaneous spikes in a 0.5 s window before stimulation and doubled the result to obtain spikes s^{-1}. Spontaneous activity was quantified by counting the spikes in a 5 s window without stimulus and then dividing by five to obtain spikes s^{-1}. After verifying that the responses were normally distributed, we compared all genotypes for a given experiment by analysis of variance (ANOVA), with the genotype as the main effect, and adjusted the alpha level for planned post hoc means comparisons.

To assess the responses of live flies to volatile compounds, ~100–120 male or virgin female flies were placed in a 5 ml glass pipette (witeg Labortechnik). The pipette was then closed at each end with cotton gauze, and an air pulse (3 s) was blown through it. As controls, an empty pipette was used or a pipette loaded with 10 µl phenylacetic acid (0.1 µg $µl^{-1}$ in paraffin oil, as 1 µl drops on ten individual 2 mm^2 filter papers). The responses were quantified by counting all of the spikes in a 1 s window from 500 ms after the odour stimulus trigger and then subtracting the number of spontaneous spikes in a 1 s window before stimulation. To assess the responses to *D. melanogaster* cuticular hydrocarbons, we prepared extracts in 50 µl CH_2Cl_2 as described below (except without the *n*-C13 standard) and then evaporated the solvent under N_2 and diluted the extract in paraffin oil to a concentration of 10 fly equivalents $µl^{-1}$. These extracts (1 µl) (or control stimuli) were placed on the tip of a borosilicate glass capillary (World Precision Instruments) and brought into close proximity (~5 mm) to the antenna. The changes in spiking frequency were quantified by measuring the spontaneous spiking frequency in spikes s^{-1} in a 3 s window before the stimulus was brought close to the antenna and then subtracting this value from the spiking frequency in a 3 s window when the stimulus was placed close to the antenna. This second 3 s window typically started 3–5 s after stimulus placement, a time frame when the responses to phenylacetic acid were most robust.

Extract preparation and chemical analysis. As phenylacetaldehyde and phenylacetic acid are polar compounds, we used CH_2Cl_2 for all extractions. *D. melanogaster* extracts were prepared by incubating five to ten 5-day-old flies for 5 min in vials containing 50 µl CH_2Cl_2 and 100 ng *n*-C13 (as an internal standard) at room temperature. After the flies were removed, the extracts were stored at −20 °C until analysis. For standard fly food and fruit extracts, 2 g material was crushed in 20 ml vials containing 4 ml CH_2Cl_2 and 200 ng *n*-C13 as an internal standard. After vortexing for 10 min at room temperature, the extracts were filtered through glass wool and concentrated to ~100 µl under a gentle flow of N_2. The extracts were stored at −20 °C until analysis.

Because of the difficulty of detecting phenylacetic acid and phenylacetaldehyde at low concentration in the extracts, we tested three column types with different polarities: a CP-Sil 5 CB (apolar type, 25 m × 0.25 mm internal diameter, 0.12 µm film thickness; Varian), a CP-Wax 58 CB (polar type, 25 m × 0.25 mm internal diameter, 0.20 µm film thickness; Varian) and a VF-1ms (medium polarity type, 20 m × 0.15 mm internal diameter, 0.15 µm film thickness; Varian). Only the last two columns gave satisfactory quantitative results, and these were used for all subsequent analyses. The extracts were analysed using a GC-MS-QP2010 apparatus (Shimadzu) in splitless mode, fitted with a VF-1ms (*D. melanogaster* extracts) or a CP-Wax 58 CB (standard fly food, banana and prickly-pear extracts) fused silica capillary column. The columns were held isothermally at 40 °C for 2 min, then the temperature was programmed to increase at a rate of 3 °C min^{-1} to 240 °C (CP-Wax 58CB) or 300 °C (VF-1ms). Helium was used as the carried gas at a linear velocity of 47 cm s^{-1}. The injector port was set at 280 °C. The mass spectrometer was operated at 70 eV, and scanning was performed from 29 to 600 AMU at 0.5 scans s^{-1}. The injection split was opened 1 min after the injection. Phenylacetic acid and phenylacetaldehyde were identified using their retention time and their fragmentation patterns; diagnostic ions were compared with both the NIST/EPA/NIH Mass Spectral Library and the mass spectrum of synthetic chemical standards (Sigma-Aldrich) analysed under the same conditions. For quantitative analyses of phenylacetic acid and phenylacetaldehyde, the response factor was determined for each of the compounds and *n*-C13 at 0.1, 0.5, 1, 5 and 10 ng on both types of column. For analysis of extracts from flies grown on minimal medium, late second or young third instar larvae reared on standard food medium were washed six times in distilled water to remove any traces of medium. Larvae were then transferred to a minimal growth medium (0.1 M sucrose and 1% agarose). At emergence, adults were separated by sex and aged in groups of 20 flies on minimal growth medium for 5 days, before extraction as described above.

Courtship assays. Male and virgin female flies were collected at eclosion. They were kept in vials, individually for subjects or in groups of 10 for objects, for 5–9 days before behavioural assays. The vials contained fresh food and were kept under a 12 h light and 12 h dark cycle at 25 °C. Behavioural assays were performed at approximately the same time each morning. Single-pair courtship tests were performed in round observation chambers (1.2 cm in diameter and 0.4 cm deep, with nine-chamber plexiglass courtship wheels) under far-red light (to eliminate the contribution of visual cues) at 25 °C. For most experiments, object females (or males) were decapitated with a clean razor blade (to avoid any reciprocal interaction during courtship) and were left to 'recover' for ~10 min before introduction into the courtship chamber. We also tested males for their courtship behaviour in more natural conditions: using intact live virgin Canton-S females, together with ~90 mg fly food medium (corresponding to approximately one-quarter of the courtship chamber volume). Male courtship behaviour towards these different types of object was recorded for 10 min with an HDR-SR10 digital video camera (Sony). After recording, videos were analysed by a researcher who was blinded to the genotypes, using Annotation software (SaySoSoft). The courtship index was calculated as the percentage of time that a male courted the object during a 10-min period. Female copulation behaviour was quantified by direct observation for 1 h without video recording: copulation latency represents the time to the beginning of copulation from the moment that the virgin female and the male are placed in the chamber; copulation success is the percentage of flies that copulate; and copulation duration is the total time of copulation from the start to the end of copulation.

For perfumed assays, the courtship chamber was placed on top of an identical chamber, and the chambers were separated by muslin gauze to avoid direct contact between the flies in the top chamber and the chemical stimuli in the bottom chamber (food, 50 ± 2 mg standard fly food; solvent, 10 µl paraffin oil (on a filter paper or aluminium foil pad); phenylacetic acid, 10 µl ~35 µg $µl^{-1}$ solution in

paraffin oil (that is, ~2.5 μmol total odour); ethyl butyrate, 10 μl 1% (v/v) solution in paraffin oil (that is, ~0.8 μmol total odour)). Single object males were placed in the upper chamber with a killed intact virgin wild-type female at 25 °C. The female had been anaesthetized with CO_2, placed in an Eppendorf tube and killed by submerging the tube in liquid nitrogen. The female was then warmed for ~10 min at 25 °C in a Petri dish before being placed in the courtship chamber. Males court killed objects only at low levels, facilitating the determination of the enhancing effect of perfuming.

Olfactory assays. Male olfactory responses were tested using an adapted Y-maze assay[35]; in brief, three-way plastic tube connectors (Reactolab) were used to join three glass vials by way of 1 ml pipette tips that pierced the cotton vial tops, forming a tightly sealed Y maze. The narrow ends of the pipette tips were cut and oriented in each vial top to form one 'loading' vial and two 'trap' vials, which contained 40 μl odour (10% (v/v) acetic acid in water (that is, ~70 μmol total odour) or ~35 $\mu g\,\mu l^{-1}$ phenylacetic acid in paraffin oil (that is, ~10 μmol total odour)) or 40 μl corresponding solvent on filter paper. Ten 5–9-day-old males (starved for 18–21 h in glass tubes with water on filter paper) were introduced without CO_2 anaesthesia into the loading vial and were allowed 2 h at 25 °C to choose to enter the trap vial containing the odour or the solvent. The resultant olfactory index was obtained with the following formula: (number in the odour tube − number in the solvent tube)/total number of loaded males.

Projection neuron analysis. Projection neuron images (275) from four different sources were brought into a common reference space for analysis[22,36–38]. The common template (Cell07) was from ref. 22, so 236 projection neuron images from that study did not require further processing. The anti-Discs large channel of 34 confocal images from ref. 38 was registered to a single female template brain (FlyCircuit ID 6475, FC6475), which was chosen for good quality staining and imaging, using the CMTK toolkit (http://www.nitrc.org/projects/cmtk) as described previously[23]. The FC6475 template brain was then registered to the Cell07 brain using landmarks registration based on 24 manually chosen anatomical landmarks visible in both anti-Discs large and nc82 staining. This landmarks registration used the pnreg command of the IRTK toolkit (http://www.doc.ic.ac.uk/~dr/software), which uses nonlinear third-order B-spline registration[39]. The fiducial registration error, measured as the root mean squared deviation, was 5.1 μm after affine registration and 2.4 μm after warping registration, corresponding to per axis accuracies of 2.9 and 1.4 μm, respectively. The final per axis registration accuracy for independent landmarks (not used during the registration) was 3.3 μm, which is comparable to that of previous studies[22,24].

Three VL2a projection neuron images from ref. 37 were registered to the Cell07 template by choosing 12–14 landmarks in the nc82 channel present in each stack. Landmarks registration used the pnreg command of IRTK. Two VL2a projection neuron images from ref. 36 were registered to the Cell07 template using 10–14 landmarks. Although those brains had weak nc82 staining, the only reliable marker was GH146-GAL4-driven expression of a CD2 reporter. We therefore used a two-channel confocal image of an nc82-stained brain with GH146-driven mCD8:GFP expression that had been registered by way of its nc82 channel to the Cell07 template to help choose landmarks. Landmarks registration again used the pnreg command of IRTK. The fiducial registration error (root mean squared deviation) for the five brains varied between 3.6 and 4.9 μm (affine) and 1.8 and 3.1 μm (warp).

Neuronal tracing was carried out in Amira (http://www.amira.com) with the hxskeletonize plug-in[40]. The three-dimensional coordinates of neuronal tracings were then transformed from their respective original image coordinates using the CMTK gregxform tool (FlyCircuit images → FC6475 template) and the IRTK ptransformation tool (FC6475 → Cell07, three VL2a images → FC6475). The underlying tools were called using custom code written in R (http://www.r-project.org), which was also used to analyse the transformed neuronal tracings (using the AnalysisSuite R package)[22]. The final visualization was carried out in Amira using Tcl scripts to load, show/hide and colour neuron tracings and to take snapshots. R and Tcl source code, landmark files, template brain images and neuronal tracings will be available on publication at the Jefferis laboratory website (http://flybrain.mrc-lmb.cam.ac.uk).

Analysis of axonal overlap. The degree of overlap between the axon terminals of different projection neurons was measured by making use of the three-dimensional convex hull of each terminal (using the Qhull library[41] as exposed by the R geometry package). It may help to note that for a set of two-dimensional points in the plane, the convex hull can be obtained by stretching an elastic band to encompass the whole object and then releasing it. To obtain an overlap score for a projection neuron pair (A,B), we calculated three convex hulls, $H(A)$, $H(B)$ and $H(A,B)$, where $H(A,B)$ is the convex hull for all of the points in A and B. We then calculated a normalized overlap score as $s(A,B) = (H(A) + H(B) - H(A,B))/(H(A) + H(B))$.

If A and B are identical (that is, complete overlap), the score will be 0.5. Less overlap will result in lower scores, with negative scores when the amount of intervening space between the axon terminals exceeds the overlap (if any). We first calculated an overlap score for all 275 neurons in the data set. We then aggregated the scores for all pairwise combinations of the 46 projection neuron classes in the data set and calculated the median score for each combination. This resulted in a symmetrical distance matrix with $46 \times 45/2 = 1{,}035$ unique off-diagonal entries. The median overlap score for VL2a and VA1lm projection neurons was 0.224, which was at the 97.7th centile: that is, the overlap between these two classes was among the strongest 2.3% in the data set. VL2a was the neuronal class with the strongest overlap with VA1lm (and vice versa). Cluster analysis of these data was performed with Ward's method, using the hclust function of R. Overlap scores, s, were converted to a distance, d, suitable for clustering by the simple transform $d = 0.5 - s$.

The VL2a projection neuron image data were obtained in separate studies from the bulk of the projection neuron data, so it is natural to ask whether this could have had some effect on our analysis. However, the consistent results for VL2a projection neuron images obtained from two different laboratories argue very strongly against this possibility. Visual inspection indicated that there was excellent overlap between the VL2a neurons from the two sources, and the pairwise overlap scores between and within the two groups were almost identical (median 0.284 and median 0.301, corresponding to the 98.0th and 98.8th centiles in Supplementary Fig. 4b). As an additional check, we repeated the axon overlap analysis and clustering with affine registered VL2a neurons (affine registration is more robust, although it is less accurate in the ideal situation). This had a negligible effect on the VL2a/VA1lm median overlap score (0.197 and 0.224, corresponding to the 96.2th centile and 97.7th centile, respectively) and had no effect on the clustering results (G.S.X.E.J., data not shown).

Phylogenetic analysis. The phylogenetic tree of selected antennal-expressed IR orthologous groups[25] was constructed using PhyML[42] and is based on the most conserved columns of an amino acid alignment generated with MUSCLE[43]. The phylogeny was rooted using IR25a. iTOL[44] was used to view and graphically edit the tree.

29. Lee, T. & Luo, L. Mosaic analysis with a repressible cell marker for studies of gene function in neuronal morphogenesis. *Neuron* **22,** 451–461 (1999).
30. Lai, S. L. & Lee, T. Genetic mosaic with dual binary transcriptional systems in *Drosophila. Nature Neurosci.* **9,** 703–709 (2006).
31. Han, D. D., Stein, D. & Stevens, L. M. Investigating the function of follicular subpopulations during *Drosophila* oogenesis through hormone-dependent enhancer-targeted cell ablation. *Development* **127,** 573–583 (2000).
32. Rong, Y. S. *et al.* Targeted mutagenesis by homologous recombination in *D. melanogaster. Genes Dev.* **16,** 1568–1581 (2002).
33. Bischof, J., Maeda, R. K., Hediger, M., Karch, F. & Basler, K. An optimized transgenesis system for *Drosophila* using germ-line-specific ϕC31 integrases. *Proc. Natl Acad. Sci. USA* **104,** 3312–3317 (2007).
34. Benton, R., Sachse, S., Michnick, S. W. & Vosshall, L. B. Atypical membrane topology and heteromeric function of *Drosophila* odorant receptors *in vivo. PLoS Biol.* **4,** e20 (2006).
35. Alcorta, E. & Rubio, J. Intrapopulational variation of olfactory responses in *Drosophila melanogaster. Behav. Genet.* **19,** 285–299 (1989).
36. Wong, A. M., Wang, J. W. & Axel, R. Spatial representation of the glomerular map in the *Drosophila* protocerebrum. *Cell* **109,** 229–241 (2002).
37. Yu, H. H. *et al.* A complete developmental sequence of a *Drosophila* neuronal lineage as revealed by twin-spot MARCM. *PLoS Biol.* **8,** e1000461 (2010).
38. Chiang, A. S. *et al.* Three-dimensional reconstruction of brain-wide wiring networks in *Drosophila* at single-cell resolution. *Curr. Biol.* **21,** 1–11 (2011).
39. Rueckert, D. *et al.* Nonrigid registration using free-form deformations: application to breast MR images. *IEEE Trans. Med. Imaging* **18,** 712–721 (1999).
40. Evers, J. F., Schmitt, S., Sibila, M. & Duch, C. Progress in functional neuroanatomy: precise automatic geometric reconstruction of neuronal morphology from confocal image stacks. *J. Neurophysiol.* **93,** 2331–2342 (2005).
41. Barber, C. B., Dobkin, D. P. & Huhdanpaa, H. The Quickhull algorithm for convex hulls. *ACM Trans. Math. Softw.* **22,** 469–483 (1996).
42. Guindon, S. & Gascuel, O. A simple, fast, and accurate algorithm to estimate large phylogenies by maximum likelihood. *Syst. Biol.* **52,** 696–704 (2003).
43. Edgar, R. C. MUSCLE: multiple sequence alignment with high accuracy and high throughput. *Nucleic Acids Res.* **32,** 1792–1797 (2004).
44. Letunic, I. & Bork, P. Interactive Tree Of Life (iTOL): an online tool for phylogenetic tree display and annotation. *Bioinformatics* **23,** 127–128 (2007).